Justin Caplan, B.A.
Department of Neurosurgery,
Johns Hopkins University,
School of Medicine,
Baltimore, Maryland

Gustavo Pradilla, M.D.
Department of Neurosurgery,
Johns Hopkins University,
School of Medicine,
Baltimore, Maryland

Alia Hdeib, B.A.
Department of Neurosurgery,
Johns Hopkins University,
School of Medicine,
Baltimore, Maryland

Betty M. Tyler, B.A.
Department of Neurosurgery,
Johns Hopkins University,
School of Medicine,
Baltimore, Maryland

Federico G. Legnani, M.D.
Department of Neurosurgery,
Johns Hopkins University,
School of Medicine,
Baltimore, Maryland

Carlos A. Bagley, M.D.
Department of Neurosurgery,
Johns Hopkins University,
School of Medicine,
Baltimore, Maryland

Henry Brem, M.D., F.A.C.S.
Departments of Neurosurgery
and Oncology,
Johns Hopkins University,
School of Medicine,
Baltimore, Maryland

George Jallo, M.D.
Departments of Neurosurgery
and Pediatrics,
Johns Hopkins University,
School of Medicine,
Baltimore, Maryland

Reprint requests:
George Jallo, M.D.,
Department of Neurosurgery,
Johns Hopkins University,
School of Medicine,
Harvey 811, 600 N. Wolfe Street,
Baltimore, MD 21287.
Email: gjallo1@jhmi.edu

Received, August 1, 2005.
Accepted, February 9, 2006.

A Novel Model of Intramedullary Spinal Cord Tumors in Rats: Functional Progression and Histopathological Characterization

OBJECTIVE: Intramedullary spinal cord tumors are difficult lesions to treat given their recurrence rate and limited treatment options. The absence of an adequate animal model, however, has hindered the development of new treatment paradigms. In this study, we describe the technique for intramedullary injection of two experimental rodent gliomas (9L and F98) and present the methodology for functional and histopathological analysis of tumor progression.

METHODS: F344 rats (n = 24) were randomized into three groups. Group 1 (n = 8) received a 5 μl intramedullary injection of Dulbecco's modified Eagle medium, Group 2 received a 5 μl intramedullary injection of 9L gliosarcoma (100,000) cells, and Group 3 received a 5 μl intramedullary injection of F98 glioma (100,000) cells. The animals were anesthetized, a 2 cm incision was made in the dorsal mid-thoracic region, and the spinous process of the T5 vertebrae was removed to expose the intervertebral space. The ligamentum flavum was removed, and an intramedullary injection was made into the spinal cord. The animals were evaluated daily for signs of paralysis using the Basso, Beattie, and Bresnahan scale and sacrificed after the onset of deficits for histopathological analysis.

RESULTS: Animals injected with 9L-gliosarcoma had a median onset of hind limb paresis at 12 $\pm$ 2.9 days. Animals injected with F98 glioma had a median onset of hind limb paresis at 19 $\pm$ 3 days. Animals injected with Dulbecco's modified Eagle medium did not show neurological deficits. Hematoxylin-eosin cross sections confirmed the presence of intramedullary 9L and F98 tumor invading the spinal cord. Control animals had no significant histopathological findings.

CONCLUSION: Animals injected with 9L or F98 consistently developed hind limb paresis in a reliable and reproducible manner. The progression of neurological deficits is similar to that seen in patients with intramedullary spinal cord tumors. These findings suggest that this model mimics the behavior of intramedullary spinal cord tumors in humans and may be used to examine the efficacy of new treatment options for both low- and high-grade intramedullary tumors.

KEY WORDS: 9L gliosarcoma, Animal model, F98 glioma, Intramedullary spinal cord tumor

Neurosurgery 59:193-200, 2006 DOI: 10.1227/01.NEU.0000219276.44563.DA www.neurosurgery-online.com

The prognosis of intramedullary spinal cord tumors (IMSCTs) remains poor (9) mainly because of their infiltrative nature, high recurrence rate, and limited treatment options (13, 38, 41, 42). These lesions generally arise from glial or ependymal cells, represent 5 to 25% of all intraspinal tumors, and are more prevalent in children than adults (1, 19, 32).

Surgical resection still remains the standard of care for these patients, with total gross resection as the operative aim (9, 20, 23, 32, 37, 38). Complete gross resection, however, can be difficult given the infiltrative nature of IMSCTs, the presence of surrounding normal cord, and the absence of clear surgical planes between cancerous and normal spinal cord tissue (23, 32). Although surgical intervention is aimed at preventing further progression of neurological deficits, deterioration eventually occurs (37).

The use of radiotherapy or chemotherapy for the treatment of IMSCT remains controversial. Radiotherapy is often used as an adjunct to surgical resection for high-grade tumors (37). The reported efficacy of this strategy, however, varies significantly between centers and is influenced strongly by tumor grade (20, 23, 38). Ten-year survival rates for patients with low-grade astrocytomas receiving postoperative radiation therapy is as low as 40 to 50% (11, 17, 40) and as high as 89 to 91% (25, 27). Two-year survival rates for patients with high-grade astrocytoma receiving postoperative radiation therapy is often 0% (12, 14, 25, 27, 29), but some centers have reported rates as high as 40% (40).

The current role of chemotherapy is also limited (32). Physiological barriers such as the blood-brain barrier, formed by tight junctions of the cerebral capillary endothelial cells, the blood-cerebrospinal fluid barrier, and the blood tumor barrier (26, 33), limit the permeability of drugs delivered to the central nervous system. To circumvent these barriers, several methods have been developed to deliver therapeutics directly to the site of the tumor and are currently used in the treatment of malignant brain tumors and other malignancies (26). To adequately test the safety and efficacy of these and other novel approaches in the setting of IMSCTs, a reliable and readily reproducible animal model must be developed.

Although many intracranial animals models exist (10, 18, 21, 36, 45), a search of the literature reveals only one previous attempt to create an animal IMSCT model (35). In this study, Salcman et al. (35) injected adult mongrel dogs with an intramedullary tumor cell suspension of a canine gliosarcoma and measured the time to onset of paresis. The absence of a detailed standardized record of motor function and the use of dogs, which are expensive and limited experimental subjects, have limited the applicability of this model in preclinical testing.

We have previously developed a model of IMSCT in rabbits (28). This model is suitable for dose escalation/toxicity studies, but the limited availability of monoclonal antibodies for histopathological and molecular analysis, higher cost, and the existence of only one nonglial transplantable tumor cell line (VX2 carcinoma) constitute limiting factors.

Development of a rodent model of IMSCT using glial cell lines would facilitate biological and histopathological studies, lower cost, and increase accessibility to the model. Established rodent tumor lines of intracranial glial tumors commonly used, such as the 9L gliosarcoma and the F98 glioma that are syngeneic to Fischer 344 rats, are ideal candidates for intramedullary implantation given their predictable growth rate and their aggressive nature (4). In this study, we present a novel rat model of IMSCTs using 9L gliosarcoma and F98 glioma and discuss the methodology, histopathological features, and functional correlation of spinal cord invasion with the loss of hind limb motor function after tumor implantation.

MATERIALS AND METHODS

Experimental Design

Twenty-four Fischer 344 rats were randomized into three experimental groups. Animals in the first group (n = 8) received a 5 μl intramedullary injection containing Dulbecco's modified Eagle medium (DMEM) and were used as controls. Animals in the second group (n = 8) received a 5 μl intramedullary injection containing 100,000 9L gliosarcoma cells in 5 μl media. Animals in the third group (n = 8) received a 5 μl intramedullary injection containing 100,000 F98 glioma cells in 5 μl media. The hind limb motor function of the animals was assessed as described below, and the animals were sacrificed after onset of paraparesis for histopathological analysis.

Animals

Female Fischer 344 rats weighing 150 to 200 g were obtained from Charles River Laboratories (Wilmington, MA). They were housed in standard facilities and given free access to water and rodent chow. All of the rats were treated in accordance with the policies and principles of laboratory animal care of the Johns Hopkins University School of Medicine Animal Care and Use Committee.

Tumor Lines

The 9L gliosarcoma was obtained from Dr. Marvin Barker at the University of California–San Francisco Brain Tumor Research Center (San Francisco, CA). The F98 glioma was obtained from Dr. Rolf F. Barth (Ohio State University, Columbus, OH). Cell lines were grown in DMEM (Gibco, Invitrogen Corporation, Grand Island, NY) with 4.5 g/L glucose, supplemented with 10% fetal bovine serum and penicillin/streptomycin. A tumor suspension was prepared by suspending 100,000 cells in 5 μl DMEM.

Surgical Technique

Rats were anesthetized with an intraperitoneal injection (0.4–0.6 ml) of a stock solution containing ketamine hydrochloride (25 mg/ml; Hospira, Inc., Lake Forest, IL), xylazine (2.5 mg/ml; Phoenix Pharmaceutical, Inc., St. Joseph, MO), and 14.25% ethanol in normal saline. Animals were placed on a sterile field, and their backs were shaved and prepared with a betadine solution. The spinous process of T5 was identified, and a 2-cm longitudinal incision was made over the dorsal mid-thoracic region. The underlying fascia and the paravertebral muscles were retracted laterally, the spinous process of T5 was removed with rongeurs, and the ligamentum flavum was removed, exposing the intervertebral space. The cell suspension was injected through the dorsal intervertebral space with a 26-gauge Hamilton syringe (Hamilton Company, Reno, NV) (*Figs. 1* and *2*). The needle was advanced until the dorsal aspect of the vertebral body was felt and then retracted slightly (1–2 mm). Penetration of the spinal cord was confirmed by monitoring a lower extremity motor reflex after needle insertion. Wounds were closed with surgical staples, and analgesia was provided with an intraperitoneal injection of 0.2 ml of 0.02 mg/ml buprenorphine (Abbott Laboratories, North Chicago, IL) in saline.

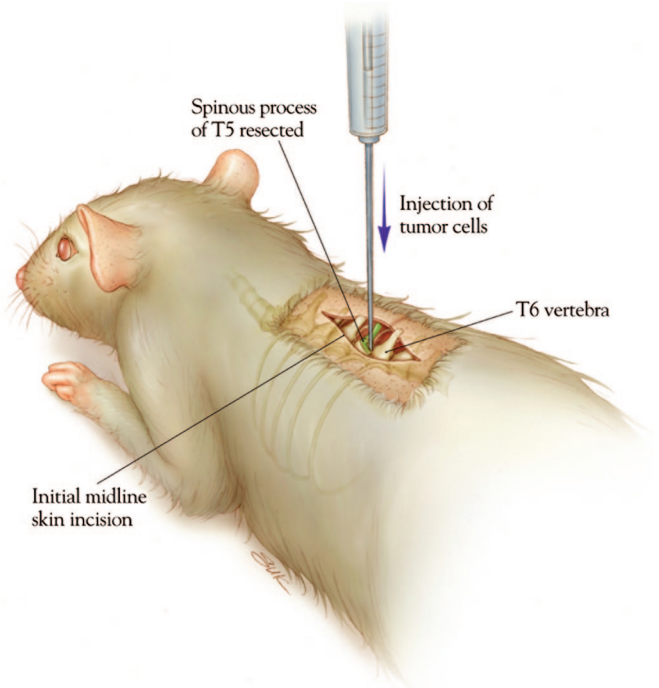

FIGURE 1. *Artist's illustration depicting the incision and surgical approach for intramedullary tumor injection in rat. The positioning of the animal, as well as the adequate angle of needle penetration for a Hamilton syringe containing tumor cell suspension, is shown. The spinous process of the T5 vertebrae removed during the approach is illustrated in* green *and shown in detail in Figure 2.*

Functional Testing

Functional testing of hind limb strength was assessed using the Basso, Bresnahan, and Beattie (BBB) scale (5, 6). Rats were placed in an open field testing area and allowed to adapt. Once the animal walked continuously, it was observed for 4 minutes and locomotion was rated using the BBB locomotor scale. The BBB scale is a 22-point scale ranging from 21 (consistent plantar stepping and coordinated gait, consistent toe clearance, predominant paw position is parallel throughout stance, consistent trunk stability, tail consistently up) to 0 (no observable hind limb movement). All animals were tested preoperatively to ensure a baseline locomotor rating of 21. Postoperatively, the animals were tested at least once every other day. Two different observers were randomly assigned to score the animals' motor function.

Euthanasia

When the functional BBB score of an animal was less than or equal to 5 (slight movement of two joints and extensive movement of the third), euthanasia was performed by CO_2 overexposure. The experiment was concluded at Day 60, and all animals in the DMEM only (control) group were sacrificed at this time.

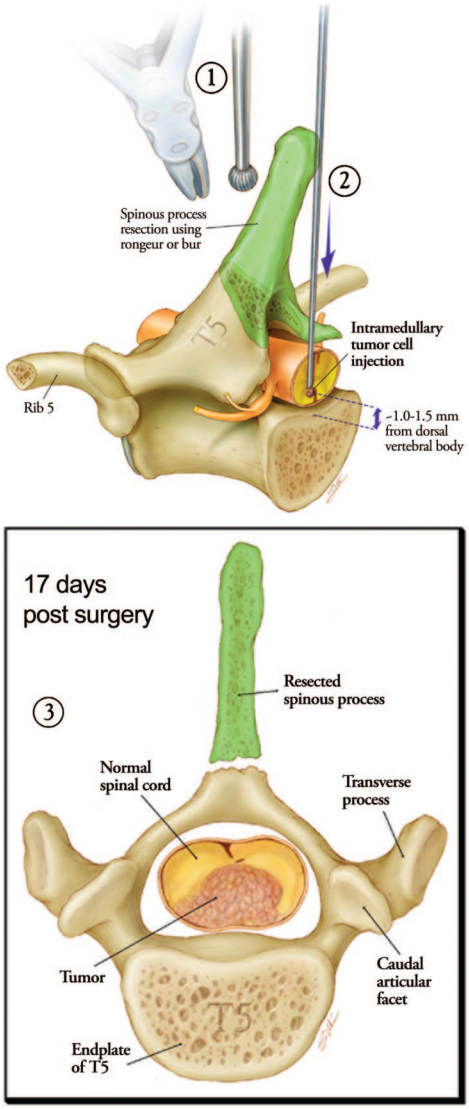

FIGURE 2. *Artist's illustration depicting 1) removal of T5 spinous process (highlighted in* green*) using rongeurs or drill; 2) intramedullary injection of tumor cell suspension. Note the relationship between the tip of needle and the posterior wall of the vertebral body and the indicated distance for needle retraction after contact with the vertebral body; 3) cross-sectional view representing the specimen 17 days after tumor implantation. Invasion and compression of a normal spinal cord at this time point is represented.*

Histopathological Analysis

After sacrifice, the spinal column of each animal was exposed, and a segment encompassing all macroscopically visible tumor was excised en bloc and placed in 4% formalin in phosphate-buffered saline. At the completion of the study, all spines were placed in hydrochloric acid for decalcification. Collected specimens included the surgical level and two vertebral segments above and below the level of tumor implantation. Three decalcified thoracic spine sections (2 mm each) were sliced axially (two sections through visible tumor, one

section through normal tissue) and embedded in paraffin. Five slides (10 μm thick) were obtained from each section for hematoxylin-eosin staining.

Statistical Analysis

In this study, a BBB functional score of less than 5 was the primary end point and thus the threshold for sacrifice. Survival times were compared between groups using the log rank (Mantel-Cox) test in Kaplan-Meier nonparametric analysis of survival. SPSS 8.0 (SPSS Inc., Chicago, IL) software for Windows was used for the statistical analyses. Results of the BBB score are expressed as mean $\pm$ standard error of the mean. Results for median survival are reported as median $\pm$ standard error of the mean. Euthanized animals in each group were recorded with "0" as its functional score for each day postsacrifice.

RESULTS

Functional Progression

A total of 24 rats received a 5 μl intramedullary injection. Animals in the first group (controls) had no significant functional deficits through the course of the study (Day 60). On postoperative Day 11, control animals had a BBB score of 18.25 $\pm$ 0.25, animals from the second group (9L) had a mean score of 8.4 $\pm$ 2.68, and animals in the third group (F98) had a mean score of 9.5 $\pm$ 0.68 (*Fig. 3*).

Animals receiving 9L had a median survival of 12 $\pm$ 2.9 days. Animals receiving F98 had a median survival of 19 $\pm$ 3.4 days. There was a significant difference between median survival of the 9L and F98 groups ($P = 0.034$, Mantel-Cox log rank test). There was no mortality among control animals (9L versus controls $P < 0.0001$, F98 versus controls $P = 0.0001$) (*Fig. 4*).

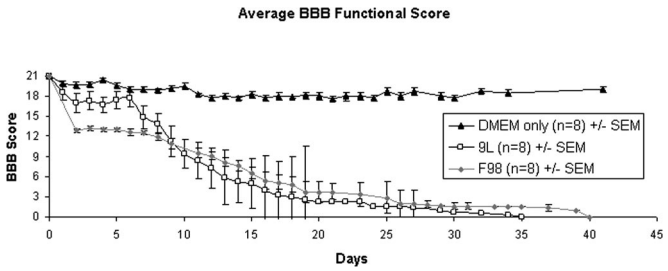

FIGURE 3. *Line graph depicting the mean BBB score of each group over time in days. Control animals* (solid circles) *show a sustained BBB score throughout the study. Animals implanted with 9L gliosarcoma* (empty squares) *show a progressive decline in motor function that starts approximately 7 days after implantation. Animals implanted with F98 glioma* (solid triangles) *show a progressive but slower decrease in motor function when compared with 9L animals. Error bars are* $\pm$ *standard error of the mean.*

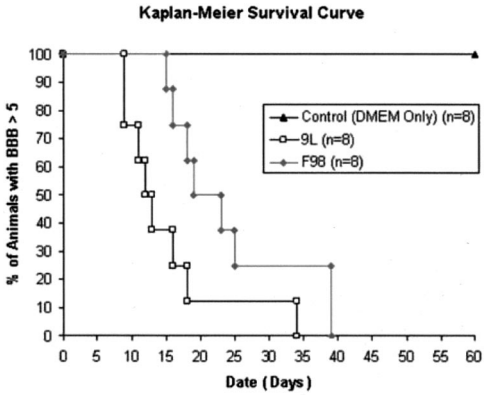

FIGURE 4. *Kaplan-Meier graph showing the onset of paralysis (BBB function score < 5). Control animals* (solid circles) *did not show onset of paralysis throughout the study. Animals implanted with 9L* (empty squares) *showed faster onset of paralysis when compared with animals implanted with F98* (solid triangles).

Histopathology

Examination of control animals revealed no significant findings (*Fig. 5*). Histopathological examination of those animals injected with 9L gliosarcoma revealed highly cellular, well-circumscribed lesions invading the white matter with finely fibrillary backgrounds, and compression of the gray matter (*Fig. 6*). Within the tumors, cellular nuclei were polymorphic with bizarre nuclear patterns; occasional multinucleated cells were observed, with clearly identified mitotic figures. Endothelial proliferation was evident, and alternating areas of angiogenesis and necrosis were frequently observed. Histopathological examination of animals injected with F98 glioma revealed infiltrative lesions, with a high degree of white and gray matter invasion (*Fig. 7*); abundant necrosis was consistently observed with replacement of normal structures

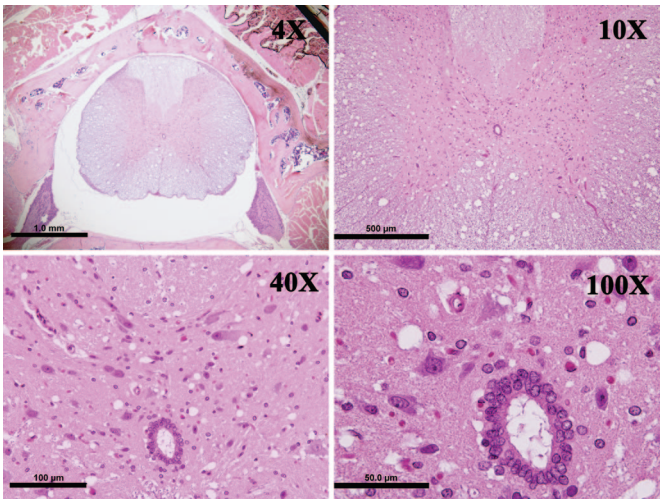

FIGURE 5. *Microphotographs of cross section of the spinal cord of a rat injected with DMEM (control) and stained with hematoxylin-eosin.* Top left *image shows a normal spinal cord in situ at* $\times 4$ *magnification.*

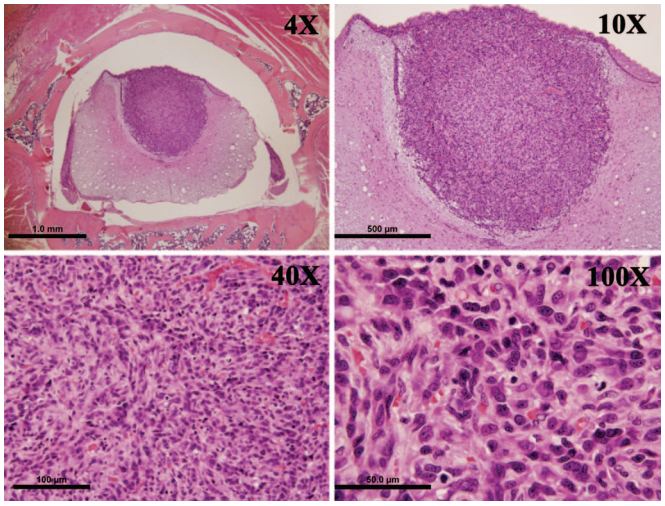

FIGURE 6. *Microphotographs of cross section of the spinal cord of a rat injected with 9L gliosarcoma and stained with hematoxylin-eosin. The concentric nature of 9L gliosarcoma is readily apparent, and compression of normal spinal cord tissue can be appreciated.*

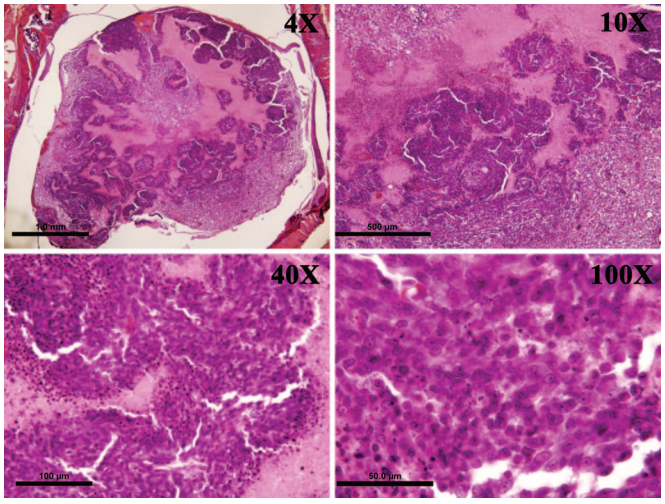

FIGURE 7. *Microphotographs of cross section of the spinal cord of a rat injected with F98 glioma and stained with hematoxylin-eosin. The highly infiltrative nature of this tumor is shown, and extensive loss of normal cytoarchitecture is observed.*

with scar tissue. Endothelial proliferation was scarce with limited angiogenesis.

DISCUSSION

In this study, we present a novel model of IMSCTs in rats using two rodent glioma cell lines, describe the methodology for tumor implantation, and define its functional and histopathological progression. We found that animals implanted with 9L and F98 had a median onset of hind limb paresis of 12 and 19 days, respectively. The progression of hind limb deficits observed in the animals implanted with tumor adequately correlates with the decline in function observed in patients with IMSCTs. Animals undergoing sham surgery recovered without incident and displayed no significant decline in hind limb function.

The 9L gliosarcoma is one of the most popular rat brain tumor models (2, 3). It was developed by Benda et al. (7) and Schmidek et al. (39) in CD Fischer rats through weekly intravenous injections of methylnitrosourea for 26 weeks and is typically described as a sarcomatous well circumscribed lesion (3) with highly immunogenic potential (8, 15, 31) and marked angiogenic activity (44). The F98 glioma is also widely used in neuro-oncology for intracranial implantation in syngeneic rats. It was developed by Ko et al. (24) in CD Fischer rats using a single intravenous injection of N-ethyl-N-nitrosourea administered to a pregnant animal on the 20th day of gestation. F98 develops as an infiltrative tumor with low immunogenic potential (43) and moderate angiogenic activity. Both cell lines are considered good models of anaplastic glioma (4).

The aggressive behavior displayed by 9L and F98 after intramedullary implantation correlates well with their progression in intracranial models (16, 22, 34). Animals receiving 9L exhibit a more rapid onset of paraparesis after an intramedullary challenge and have lower median survival rates after intracranial implantation when compared with animals implanted with F98 under the same experimental settings. The availability of two different tumor lines with different progression rates gives the investigator the option of selecting the model that best suits the needs of the experimental design.

Furthermore, the different histopathological presentation of these tumors provides a better representation of the variability observed in the human disease. Whereas the 9L is typically well circumscribed and grows with an expansive pattern that causes rapidly progressive cord ischemia, edema, and subsequent necrosis, F98 is very infiltrative, causes extensive necrosis and disruption of the normal cytoarchitecture (43), and exhibits a significantly slower rate of decline in motor function when compared with 9L. Such pathological differences have obvious implications for evaluating treatment options. This model offers the opportunity to explore the efficacy of treatments against two distinctive, yet commonly seen, pathological characterizations.

In considering the diverse cellular populations present in the normal spinal cord, it can harbor the full spectrum of central nervous system neoplasms, including astrocytomas, oligodendrogliomas, ependymomas, mixed gliomas, and mixed glial-neuronal tumors. The frequency and behavior of these tumors, however, tends to differ in the spinal cord when compared with the brain. For instance, myxopapillary ependymomas and gangliocytic paragangliomas, which are typically found in the cauda equina, are rarely found in the brain as primary lesions, and the relative frequency of certain primary spinal cord tumors differs from the frequency reported for the same tumors in the brain. Major differences can also be found in the type of IMSCTs present in pediatric patients when compared with adults. A comprehensive study on the surgical pathology of IMSCTs (30) showed that, al-

though ependymomas account for more than half of all IMSCTs in adults, they represent only 16% of IMSCTs in children, in whom fibrillary astrocytomas seem to be the most common type. Gangliogliomas and related neuronal-glial tumors are also common in children (35%), but are rare in adults (6%). Pilocytic astrocytomas, oligodendrogliomas, and mixed gliomas with oligodendrogliomatous characteristics seem to be unusual IMSCT for both children and adults. This variability in histopathological presentation must be addressed when designing experimental studies to assess novel interventions and must be considered in the development of an adequate animal model of the disease. The use of 9L and F98 provides biological and histopathological variability and, using the same methodology, other cell lines can be implanted, including human tumors in nude rodents.

Furthermore, as opposed to the usual testing conditions of intracranial tumor models, agents tested for IMSCTs will have to be delivered to the tumors without compromising the integrity of the spinal cord, and their impact can be measured by tumor size, survival, as well as by motor function. Similarly, treatment strategies that involve local drug delivery are limited by the size of the spinal cord, which warrants small drug/vehicle sizes/volumes. Moreover, the impact of these strategies is also affected by the nature and degree of surgical manipulation of the spinal cord, which is substantially different from the surgical manipulation that is required for intracranial models.

The ease of reproducibility and convenience of rats as the experimental animal make our model ideal for preclinical testing of novel therapeutics. Unlike previous IMSCT models whose only functional analysis is time to paralysis, the model presented allows for graded characterization of deficit onset and advanced molecular analysis. A shortcoming was observed in the initial experimental design when despite adequate randomization of animals allocated to receive either medium or tumor cell injection, the observers assigned to determine BBB scores could not control for the gross differences in motor function present at later stages of the experiments between animals implanted with tumor and controls, which decreased the impact of the blinding, and therefore we cannot consider the study to be truly blinded. Nonetheless, using the model described in this study, we proceeded to test intramedullary cytotoxic agents in our laboratory in a blinded, randomized fashion, and we have found the model to be optimal in differentiating dose-dependent responses, and therefore we recommend a blinded, randomized experimental design.

A common observation related to the methodology involves the postoperative drop observed on Day 2 after tumor implantation, which constitutes an artifact of the aforementioned methodology that places animals in the lowest scoring bracket of displayed functions and represents a weakness of our adaptation of the BBB scoring system. A score of 14 is the highest score, which incorporates rotated paw position during locomotion during initial contact with the surface as well as just before it is lifted off at the end of stance and represents a limitation in the adaptation of the BBB scale to our experimental settings. As such, the drop represents the decrease from the preoperative score to the post-tumor injection score as the result of rotated paws during locomotion, whereas other, higher ranked motor functions were still intact. Because the scores do not change appreciably over the first 7 days, this initial decline is likely to be the result of surgical manipulation during tumor implantation rather than tumor progression and bears no clinical significance because the scores remained at this level until tumor growth had progressed to the point of producing observable deficits, at a rate comparable with that of 9L-injected animals. The maintained level of function was high enough that motor deficits that significantly impaired motor function were not present.

We have previously described the technique for intramedullary injections in a rabbit IMSCT model, which, in consideration of the size of the rabbit spinal cord, is ideal for radiographic characterization of IMSCTs and for testing of drug delivery and image guided devices (28). Together, both models facilitate preclinical testing of therapeutics and devices for the treatment of IMSCTs.

In conclusion, this new model of IMSCTs provides reliable and reproducible methodology, correlates well with the human disease, and will be a useful tool in preclinical testing of novel treatment options.

REFERENCES

1. Balmaceda C: Chemotherapy for intramedullary spinal cord tumors. **J Neurooncol** 47:293–307, 2000.
2. Barker M, Deen DF, Baker DG: BCNU and X-ray therapy of intracerebral 9L rat tumors. **Int J Radiat Oncol Biol Phys** 5:1581–1583, 1979.
3. Barker M, Hoshino T, Gurcay O, Wilson CB, Nielsen SL, Downie R, Eliason J: Development of an animal brain tumor model and its response to therapy with 1,3-bis(2-chloroethyl)-1-nitrosourea. **Cancer Res** 33:976–986, 1973.
4. Barth RF: Rat brain tumor models in experimental neuro-oncology: The 9L, C6, T9, F98, RG2 (D74), RT-2 and CNS-1 gliomas. **J Neurooncol** 36:91–102, 1998.
5. Basso DM, Beattie MS, Bresnahan JC: A sensitive and reliable locomotor rating scale for open field testing in rats. **J Neurotrauma** 12:1–21, 1995.
6. Basso DM, Beattie MS, Bresnahan JC: Graded histological and locomotor outcomes after spinal cord contusion using the NYU weight-drop device versus transection. **Exp Neurol** 139:244–256, 1996.
7. Benda P, Someda K, Messer J, Sweet WH: Morphological and immunochemical studies of rat glial tumors and clonal strains propagated in culture. **J Neurosurg** 34:310–323, 1971.
8. Blume MR, Wilson CB, Vasquez DA: Immune response to a transplantable intracerebral glioma in rats, in Sane K, Ishi S, LeVay D (eds): *Recent Progress in Neurological Surgery*. Amsterdam, Excerpta Medica, 1974, pp 129–134.
9. Bowers DC, Weprin BE: Intramedullary spinal cord tumors. **Curr Treat Options Neurol** 5:207–212, 2003.
10. Carson BS, Anderson JH, Grossman SA, Hilton J, White CL 3rd, Colvin OM, Clark AW, Grochow LB, Kahn A, Murray KJ: Improved rabbit brain tumor model amenable to diagnostic radiographic procedures. **Neurosurgery** 11: 603–608, 1982.
11. Chun HC, Schmidt-Ullrich RK, Wolfson A, Tercilla OF, Sagerman RH, King GA: External beam radiotherapy for primary spinal cord tumors. **J Neurooncol** 9:211–217, 1990.
12. Cohen AR, Wisoff JH, Allen JC, Epstein F: Malignant astrocytomas of the spinal cord. **J Neurosurg** 70:50–54, 1989.

13. Constantini S, Miller DC, Allen JC, Rorke LB, Freed D, Epstein FJ: Radical excision of intramedullary spinal cord tumors: Surgical morbidity and long-term follow-up evaluation in 164 children and young adults. **J Neurosurg** 93 [Suppl 2]:183–193, 2000.
14. Cooper PR, Epstein F: Radical resection of intramedullary spinal cord tumors in adults. Recent experience in 29 patients. **J Neurosurg** 63:492–499, 1985.
15. Denlinger RH, Axler DA, Koestner A: Tumor-specific transplantation immunity to intracerebral challenge with cells from a methylnitrosourea-induced brain tumor. **J Med** 6:249–259, 1975.
16. DiMeco F, Rhines LD, Hanes J: Paracrine delivery of IL-12 against intracranial 9L gliosarcoma in rats. **J Neurosurg** 92:419–427, 2000.
17. Garcia DM: Primary spinal cord tumors treated with surgery and postoperative irradiation. **Int J Radiat Oncol Biol Phys** 11:1933–1939, 1985.
18. Griffitt W, Glick RP, Lichtor T: Development of a new mouse brain tumor model using implantable micro-cannulas. **J Neurooncol** 41:117–120, 1999.
19. Isaacson SR: Radiation therapy and the management of intramedullary spinal cord tumors. **J Neurooncol** 47:231–238, 2000.
20. Jallo GI, Danish S, Velasquez L, Epstein F: Intramedullary low-grade astrocytomas: Long-term outcome following radical surgery. **J Neurooncol** 53: 61–66, 2001.
21. Jallo GI, Penno M, Sukay L: Experimental models of brainstem tumors: Development of a neonatal rat model. **Childs Nerv Syst** 21:399–403, 2005.
22. Judy KD, Olivi A, Buahin KG: Effectiveness of controlled release of a cyclophosphamide derivative with polymers against rat gliomas. **J Neurosurg** 82:481–486, 1995.
23. Kane PJ, el-Mahdy W, Singh A, Powell MP, Crockard HA: Spinal intradural tumours: Part II–Intramedullary. **Br J Neurosurg** 13:558–563, 1999.
24. Ko L, Koestner A, Wechsler W: Morphological characterization of nitrosourea-induced glioma cell lines and clones. **Acta Neuropathol (Berl)** 51:23–31, 1980.
25. Kopelson G, Linggood RM: Intramedullary spinal cord astrocytoma versus glioblastoma: The prognostic importance of histologic grade. **Cancer** 50:732–735, 1982.
26. Lesniak MS, Brem H: Targeted therapy for brain tumours. **Nat Rev Drug Discov** 3:499–508, 2004.
27. Linstadt DE, Wara WM, Leibel SA, Gutin PH, Wilson CB, Sheline GE: Postoperative radiotherapy of primary spinal cord tumors. **Int J Radiat Oncol Biol Phys** 16:1397–1403, 1989.
28. Mavinkurve G, Pradilla G, Legnani FG: A novel intramedullary spinal cord tumor model: Functional, radiological, and histopathological characterization. **J Neurosurg Spine** 3: 142–148, 2005.
29. McLaughlin MP, Buatti JM, Marcus RB Jr, Maria BL, Mickle PJ, Kedar A: Outcome after radiotherapy of primary spinal cord glial tumors. **Radiat Oncol Invest** 6:276–280, 1998.
30. Miller DC: Surgical pathology of intramedullary spinal cord neoplasms. **J Neurooncol** 47:189–194, 2000.
31. Morantz RA, Wood GW, Foster M: Macrophages in experimental and human brain tumors: Part 1–Studies of the macrophage content of experimental rat brain tumors of varying immunogenicity. **J Neurosurg** 50:298–304, 1979.
32. Parsa AT, Lee J, Parney IF, Weinstein P, McCormick PC, Ames C: Spinal cord and intradural-extraparenchymal spinal tumors: Current best care practices and strategies. **J Neurooncol** 69:291–318, 2004.
33. Raza SM, Pradilla G, Legnani FG, Thai QA, Olivi A, Weingart JD, Brem H: Local delivery of antineoplastic agents by controlled-release polymers for the treatment of malignant brain tumours. **Expert Opin Biol Ther** 5:477–494, 2005.
34. Rhines LD, Sampath P, Dolan ME, Tyler BM, Brem H, Weingart J: O6-benzylguanine potentiates the antitumor effect of locally delivered carmustine against an intracranial rat glioma. **Cancer Res** 60:6307–6310, 2000.
35. Salcman M, Botero E, Rao KC, Broadwell RD, Scott E: Intramedullary canine spinal cord tumor model. **J Neurosurg** 61:761–766, 1984.
36. Salcman M, Scott EW, Schepp RS, Knipp HC, Broadwell RD: Transplantable canine glioma model for use in experimental neuro-oncology. **Neurosurgery** 11:372–381, 1982.
37. Sandalcioglu IE, Gasser T, Asgari S, Lazorisak A, Engelhorn T, Egelhof T, Stolke D, Wiedemayer H: Functional outcome after surgical treatment of intramedullary spinal cord tumors: Experience with 78 patients. **Spinal Cord** 43:34–41, 2005.
38. Sandler HM, Papadopoulos SM, Thornton AF Jr, Ross DA: Spinal cord astrocytomas: Results of therapy. **Neurosurgery** 30:490–493, 1992.
39. Schmidek HH, Nielsen SL, Schiller AL, Messer J: Morphological studies of rat brain tumors induced by N-nitrosomethylurea. **J Neurosurg** 34:335–340, 1971.
40. Shirato H, Kamada T, Hida K, Koyanagi I, Iwasaki Y, Miyasaka K, Abe H: The role of radiotherapy in the management of spinal cord glioma. **Int J Radiat Oncol Biol Phys** 33:323–328, 1995.
41. Steinbok P, Cochrane DD, Poskitt K: Intramedullary spinal cord tumors in children. **Neurosurg Clin N Am** 3:931–945, 1992.
42. Townsend N, Handler M, Fleitz J, Foreman N: Intramedullary spinal cord astrocytomas in children. **Pediatr Blood Cancer** 43:629–632, 2004.
43. Tzeng JJ, Barth RF, Orosz CG, James SM: Phenotype and functional activity of tumor-infiltrating lymphocytes isolated from immunogenic and nonimmunogenic rat brain tumors. **Cancer Res** 51:2373–2378, 1991.
44. Weingart JD, Sipos EP, Brem H: The role of minocycline in the treatment of intracranial 9L glioma. **J Neurosurg** 82:635–640, 1995.
45. Weizsaecker M, Deen DF, Rosenblum ML, Hoshino T, Gutin PH, Barker M: The 9L rat brain tumor: Description and application of an animal model. **J Neurol** 224:183–192, 1981.

COMMENTS

Caplan et al. have presented an elegant experiment regarding the criteria for, and results of, experimentally induced intramedullary spinal cord tumor (IMSCT) in rats. The functional and histopathological aspects of tumor growth are analyzed. This is invaluable information to researchers and clinicians alike. The future is all about an understanding of the presence. The authors have demonstrated their grasp of the art of scientific investigation.

Edward C. Benzel
Cleveland, Ohio

Caplan et al. describe the development of a new IMSCT model in rats using two experimental rodent gliomas (9L and F98). In contrast to controls, intramedullary injection of 9L and F98 glioma cells produced symptomatic tumor progression within a median duration of 12 and 19 days, respectively. Tumor development was further confirmed by histopathological analysis. The illustrations and photomicrographs describing the development of this IMSCT model are outstanding. There is a paucity of models with which to study IMSCTs. The current model shows great promise to assist researchers interested in studying the growth and response to therapy of tumors within the spinal cord.

Adrian W. Laxton
James T. Rutka
Toronto, Canada

Caplan et al. describe the development of a rat model of IMSCT using either the 9L or F98 cell lines. After thoracic laminectomy, tumor cells are injected into the spinal cord and the animals are followed using a previously published clinical scoring system. The technical aspects of their model are straightforward. However, the utility of the model is unclear. Although the 9L and F98 cell lines have different growth characteristics (as an encapsulated tumor mass versus an infiltrating lesion, respectively), both essentially represent transplanted tumors. The parallels between a rat with an injected tumor and a human with an intrinsic IMSCT are tenuous, especially in regard to clinical course or examination

of clinical, anatomic, and surgical factors. It would be useful for the authors to discuss how their model may be used to explore novel or specifically targeted therapies against spinal cord tumors. In defense of this study, however, it should be noted that no useful models of rat spinal cord tumor currently exist.

Allen Waziri
Jeffrey N. Bruce
New York, New York

The authors have described a model of IMSCT in rats using the 9L and F98 cell lines. Each are established rodent tumor lines of intracranial glioma that are syngenic to Fischer 344 rats, and each show a predictable growth rate with aggressive characteristics. The authors have clearly described and characterized the model, but the concern is, as always, whether this type of animal model will truly represent the human disease and whether it will be useful for assessing treatment plans. The 9L cell line is a very aggressive gliosarcoma and does not bear much similarity to the more usual diffuse infiltrative intramedullary glioma seen in humans. The F98 model is infiltrative, but does cause extensive necrosis with a slower rate of growth than a 9L model. This model might offer more similarities, but it is critical for the investigators to be cognizant that these models do cause paralysis in an animal and great care must be taken in ensuring that the animal does not suffer.

Andrew H. Kaye
Melbourne, Australia

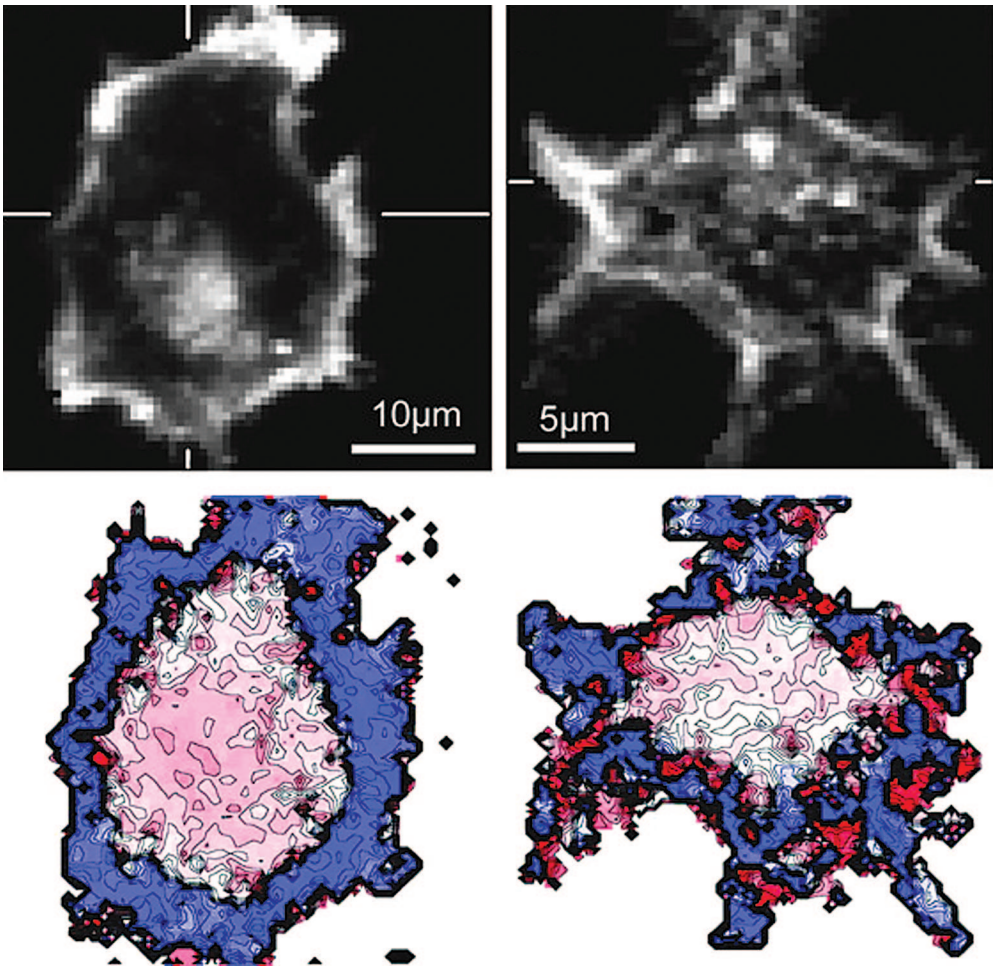

Optical methods for determining the electrical characteristics of cell-silicon junctions. *Top, confocal microscope fluorescence lock-in images of HEK293 cell (left) and rat neuron (right). Bottom, measured phase and amplitude maps of transfer functions showing adhesion regions which exhibit shallow troughs (center of images) and greater adhesion toward the periphery for the purpose of studying the strength of bi-directional (stimulation and excitation) electrical coupling between cells and silicon. (Braun D, Fromherz P: Imaging neuronal seal resistance on silicon chip using fluorescent voltage-sensitive dye.* **Biophys J** *87:1351–1359, 2004.)*